

# Analysis of Torque Sensorless Steer by Wire System Using the Bilateral Tele-Operation Concept

Esala H. Senevirathne  
Department of Electrical Engineering  
University of Moratuwa  
Moratuwa, Sri Lanka  
esala.h.senevirathne@gmail.com

A. M. Harsha S. Abeykoon  
Department of Electrical Engineering  
University of Moratuwa  
Moratuwa, Sri Lanka  
harsha@uom.lk

W. M. Theekshana G. Wijewardhana  
Department of Electrical Engineering  
University of Moratuwa  
Moratuwa, Sri Lanka  
theekshana.g.wijewardhana@gmail.com

**Abstract**—The mechanical linkage of the steering column can ideally be replaced by a bilateral controller-based steer by wire system. This paper presents an intuitive method of designing a bilaterally controlled steer by wire system based on disturbance observers and reaction torque observers. The presented system can overcome the force sensing demerits of traditional force sensors as well as the demerits of existing steer by wire systems based on bilateral control systems. Feedback torque from the steering rack to the steering wheel conveys important data about the road conditions as well as the vehicle conditions to the driver. Hence, accurate feedback to the driver is vital for smooth vehicle handling. The presented method has the capability of tuning the system as per the desire. The validity of the proposed method has been verified through simulations using real-world vehicle and controller data.

**Keywords**—Steer by wire, bilateral, disturbance observer, torque sensors.

## I. INTRODUCTION

The vehicle steering system has now evolved to a Steer by wire (SbW) system from a conventional steering system. However, the basics of steering have remained the same over the years. Road feeling is the most important feedback from the steering system [1]. It gives a sensation to the driver about the road conditions, which greatly affects the decisions made by the driver. Steering effort mainly changes with the vehicle mass and the vehicle speed. Steering effort increases as the speed and mass of vehicles increase. Therefore, power assisted steering systems were introduced to lower the steering effort to a comfortable level while preserving the important feedback. Hydraulic assisted power steering was the first to be invented, followed by electrical assisted power steering.

The SbW system was introduced due to its merits over other steering systems. The direct mechanical coupling (steering column) between the steering wheel and the steering rack is removed by the SbW system. Hence, a lot of cabin space can be saved to design a more comfortable and ergonomic interior. Furthermore, it enhanced the fuel economy and environmental friendliness of the vehicle as there is no oil associated with it. SbW systems offer the capability to improve the maneuverability and stability of the vehicle. However, the most challenging issue with SbW is to recreate the feedback torque of the road feel and steering wheel returnability. Hence, torque measurements play an important role. Usually, it is measured by a torque sensor [2].

Several studies were conducted to recreate the steering feedback torque based on parameters such as vehicle speed and steering wheel angle. A torque map-based feedback recreation methodology was developed by Zheng *et al.* [1]. Kim *et al.* used a torque damping method in order to improve steering wheel returnability and steering feel [3]. A linear quadratic regulator (LQR) controller-based torque mapping method was introduced by Fahim *et al.* [4]. Zheng *et al.* introduced a SBW system based on a bilateral control structure where the road feeling torque is estimated by using electric power steering characteristics [1].

The steer by wire systems mentioned above either use torque sensors or torque estimation methods that use torque mapping methodology to realize the road feel torque at the steering wheel actuator. Torque sensors have their demerits, such as high cost, limited range of torque sensing and size. Furthermore, their construction, which uses torsional springs, can affect the installed system dynamics [5]. Furthermore, a faulty torque sensor can cause dangerous, undesirable outcomes in SbW systems.

Torque mapping schemes do not transmit the road feel torque that has to be felt by the driver. This loss of road transparency can affect the maneuverability of the vehicle. Vibrations caused due to vehicle faults are transferred through the steering column in the conventional steering system. Such faults cannot be felt by a map-based torque recreation method.

The steering column of the conventional steering system creates a mechanical linkage between the steering wheel and the steering rack, where it transfers steering wheel motion to the steering rack. Hence, the steering column can ideally be replicated by a bilateral control system.

In a bilateral control system, the slave environment is replicated on the master side and the master environment is replicated on the slave side. To achieve the above control target, the slave side should be controlled by the force and position information of the master side and the master side should be controlled by the force and position information of the slave side [6].

The bilateral control system should transmit the input torque and angle from the steering wheel to the steering rack and the steering rack torque and angle to the steering wheel when used with SBW system. The centering torque of the vehicle wheels contributes to the steering rack torque.

This paper introduces a novel method of implementing a highly tunable torque sensorless SbW system based on the bilateral control topology. This topology has the ability to

accurately recreate the steering feedback torque in order to enhance the steering feel and response while addressing the demerits of torque sensors and shortcomings of previous studies. The force scaling ability of this bilateral system brings down the steering effort of the driver to a comfortable level while preserving the vital information of road feel. Furthermore, it can be tuned to pass the important vibrations which are associated with vehicle issues while filtering out the unnecessary vibrations.

## II. BILATERAL CONTROL

To obtain bilateral system dynamics, let's consider master and slave actuators as depicted in Fig 1.

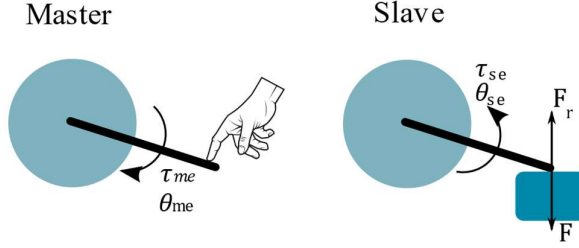


Fig 1. Bilateral control, master, and slave environments

As mentioned earlier, the slave side is controlled by the master side's torque and position information and vice versa.

If the driver exerts a torque ( $\tau_{me}$ ) on the master actuator arm, then the actuator arm rotates by  $\theta_{me}$ . If master environment impedance is  $Z_{me}$ , it can be represented as in (1) [7].

$$\tau_{me} = Z_{me}\theta_{me} \quad (1)$$

Similarly, the slave side equation can be obtained as in (2) in terms of slave side torque ( $\tau_{se}$ ), slave environment impedance ( $Z_{se}$ ), slave movement ( $\theta_{se}$ ), force on environment ( $F$ ), and reaction force on actuator ( $F_r$ ).

$$\tau_{se} = Z_{se}\theta_{se} \quad (2)$$

To achieve bilateral control, the sum of the master and slave torques ( $\tau_{me}$  &  $\tau_{se}$ ) must be zero and the master and slave positions ( $\theta_{me}$  &  $\theta_{se}$ ) must be equal as in (3) and (4)

$$\tau_{me} + \tau_{se} = 0 \quad (3)$$

$$\theta_{me} = \theta_{se} \quad (4)$$

However, depending on the requirements of the application, torque and position scalars can be used.

## III. STEERING SYSTEM MODELLING

### A. Steering Wheel and Rack Dynamics

Figure 2 depicts the conventional steering system. The mechanical linkage of the steering column between the steering wheel and the steering rack is replaced by this steer by wire system. Figure 3 depicts the physical model of the steer by wire system.

Steering wheel (master side) dynamics can be obtained as in (5), in terms of driver torque ( $\tau_{dr}$ ), steering wheel angle ( $\theta_s$ ), and steering wheel motor parameters such as motor torque ( $\tau_{sm}$ ), moment of inertia ( $J_s$ ), spring constant ( $K_s$ ), and damping coefficient ( $B_s$ ).

Similarly, rack side (slave side) dynamics can be obtained as follows in (6) in terms of rack torque ( $\tau_{rack}$ ), rack angle ( $\theta_r$ ), and steering rack motor parameters such as motor torque ( $\tau_{rm}$ ), moment of inertia ( $J_r$ ), spring constant ( $K_r$ ), and damping coefficient ( $B_r$ ).

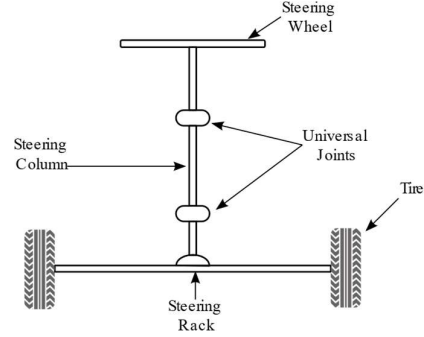


Fig 2. Conventional steering system

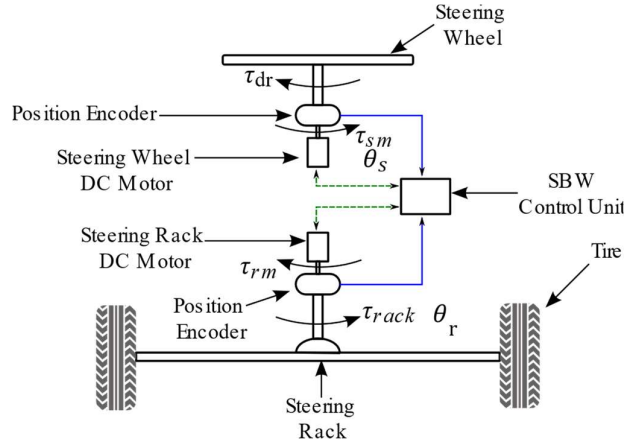


Fig 3. Steer by wire physical model

$$J_{sm}\ddot{\theta}_s = \tau_{sm} - (\tau_{dr} + K_s\theta_s + B_s\dot{\theta}_s) \quad (5)$$

$$J_{rm}\ddot{\theta}_r = \tau_{rm} - (\tau_{rack} + K_r\theta_r + B_r\dot{\theta}_r) \quad (6)$$

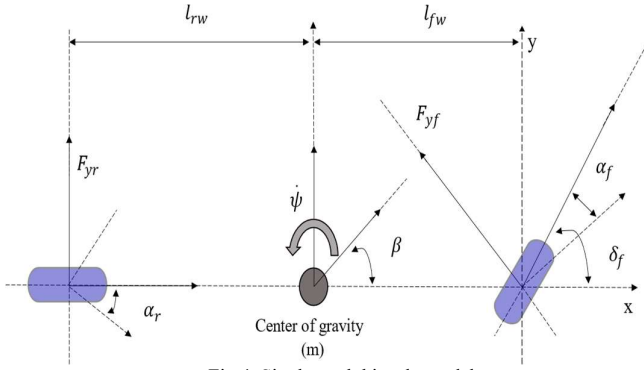


Fig 4. Single track bicycle model

### B. Single Track Vehicle Model

For the ease of vehicle dynamic analysis, the four-wheel vehicle model is simplified into a two-wheel bicycle model under the following assumptions by researchers [4].

- I. Friction force along x axis is negligible when vehicle is not braking.
- II. Constant vehicle speed.
- III. Angle of both front tires are approximately same.

The bicycle model is used to derive self-aligning torque ( $\tau_{sa}$ ) from simplified dynamics. The yaw rate ( $\dot{\psi}$ ) and vehicle body slip angle ( $\beta$ ), which are essential in self-aligning torque realization, can be derived from the bicycle model which is depicted in Fig. 4.

### C. Self-Aligning Torque ( $\tau_{sa}$ )

The front axle system converts the steering angle to front wheel angle according to the steering ratio. An opposing torque is generated at the wheels due to tire dynamics, vehicle dynamics, front wheel angle and road surface conditions. This torque always tries to center the vehicle in its traveling path. Since many factors affect this torque, the driver can get an idea (feel) about the road. This acts as a disturbance torque to the front axle system.

The state space equation of the bicycle model can be expressed as in (7) and (8). Where, yaw rate ( $\dot{\psi}$ ) and body slip angle ( $\beta$ ) are the outputs for front tire angle input ( $\delta_f$ ) [8].

For large tire slip angle ( $\alpha_f$ ), lateral force and slip angle relationship become nonlinear. However, for small tire slip angle it becomes linear. Considering small tire slip angle, then self-aligning torque can be represented as in (9).

$$\begin{aligned} \dot{x} &= Ax + Bu \\ y &= Cx \\ x &= [\dot{\psi} \quad \beta] \end{aligned} \quad (7)$$

$$\begin{aligned} A &= \begin{bmatrix} -\frac{c_{fw} l_{fw}^2 + c_{rw} l_{rw}^2}{v I_v} & -\frac{c_{fw} l_{fw} - c_{rw} l_{rw}}{I_v} \\ -1 - \frac{c_{fw} l_{fw} - c_{rw} l_{rw}}{v^2 m} & -\frac{c_{fw} + c_{rw}}{v m} \end{bmatrix} \\ B &= \begin{bmatrix} \frac{c_{fw} l_{fw}}{I_v} \\ \frac{c_{fw}}{v m} \end{bmatrix} \\ u &= \delta_f \end{aligned} \quad (8)$$

$$\tau_{sa} = -c_{fw}(t_p + t_m)[\beta + \frac{l_{fw}\dot{\psi}}{V} - \delta_f]\mu \quad (9)$$

Where,

$\tau_{sa}$  : Self-aligning torque

$c_{fw}, c_{rw}$  : Cornering stiffness of front and rear wheels

$v$  : Vehicle speed

$m$  : Vehicle mass

$l_{fw}, l_{rw}$  : Distance to cog from front and rear

$I_v$  : Vehicle yaw moment inertia

$t_p, t_m$  : Pneumatic and mechanical trails of tire

$\beta$  : Body slip angle

$\dot{\psi}$  : Yaw rate

$\delta_f$  : Front tire angle

$\mu$  : Road dry condition coefficient

### D. Driver Dynamics.

The most complex and most difficult system to model is the human model. Hence, the published research is limited regarding human steering coordination. Stiffness ( $K_{dr}$ ), damping ( $B_{dr}$ ) and inertia ( $J_{dr}$ ) of the human limb vary dynamically with the muscle group co-contraction. However, the above parameters are realized by fitting experimental data into a single spring mass damper system. Driver impedance ( $Z_{dr}$ ) can be expressed as in (10).

$$Z_{dr} = J_{dr}s^2 + B_{dr}s + K_{dr} \quad (10)$$

The above parameters are essentially limited to certain constraints, such as driver seating posture and steering wheel gripping style. Furthermore, the above model is approximately valid up to 10Hz input.

The lower bound of the parameters is zero and it is defined when there is no physical contact between the driver and the steering wheel. The upper bound values of  $K_{dr}$ ,  $B_{dr}$ , and  $J_{dr}$  are respectively 100 [Nm/rad], 1.6 [Nm s /rad], and 0.15 [kgm<sup>2</sup>]

#### IV. DISTURBANCE OBSERVERS AND TORQUE ESTIMATION

As mentioned earlier, traditional torque sensors have their own demerits. Researchers use estimation techniques to overcome those issues. The disturbance observer proposed by *Ohnishi et al.* is one such accurate estimation method of estimating disturbances in DC motors [9].

##### A. Disturbance Observer

Mechanical torque generated ( $\tau_m$ ) by a DC motor can be expressed as in (11).  $K_t$  is the torque coefficient of the motor and  $I_a$  is the armature current.

$$\tau_m = K_t I_a \quad (11)$$

Considering motor dynamics (12) can be expressed by the load torque of the motor ( $\tau_l$ ), the inertia of the motor ( $J$ ), and the angular acceleration of the motor ( $\ddot{\theta}$ )

$$\tau_m - \tau_l = J\ddot{\theta} \quad (12)$$

Load torque can be represented as in (13) in terms of inter active torque ( $\tau_{int}$ ), external torque ( $\tau_{ext}$ ), static frictional torque ( $\tau_{fric}$ ), and viscous friction torque ( $B\dot{\theta}$ ).

$$\tau_l = \tau_{int} + \tau_{ext} + \tau_{fric} + B\dot{\theta} \quad (13)$$

By adding (12) and (13) and substituting (11), following (14) can be obtained.

$$K_t I_a - J\ddot{\theta} = \tau_l = \tau_{int} + \tau_{ext} + \tau_{fric} + B\dot{\theta} \quad (14)$$

System parameters can be subjected to estimation errors and variations [10]. Hence, considering parameter variations, parameters can be expressed in terms of their variations ( $\Delta K_t$  &  $\Delta J$ ) and nominal values ( $K_{tn}$  &  $J_n$ ) as in (15) and (16).

$$K_t = K_{tn} + \Delta K_t \quad (15)$$

$$J = J_n + \Delta J \quad (16)$$

Hence (14) can be re arranged as in (17).

$$K_{tn} I_a - J_n \ddot{\theta} = \tau_{int} + \tau_{ext} + \tau_{fric} + B\dot{\theta} - \Delta K_t I_a + \Delta J \ddot{\theta} \quad (17)$$

Therefore, total disturbance on the nominal system can be expressed as in (18) and (19)

$$\tau_d = \tau_{int} + \tau_{ext} + \tau_{fric} + B\dot{\theta} - \Delta K_t I_a + \Delta J \ddot{\theta} \quad (18)$$

$$\tau_d = K_{tn} I_a - J_n \ddot{\theta} \quad (19)$$

A low pass filter with a filter coefficient  $g_d$  is used in order to compensate for the sensor noise. Hence, estimated disturbance torque ( $\hat{\tau}_d$ ) can be expressed as in (20). The cut off frequency is expressed as  $g_d$ .

$$\hat{\tau}_d = \frac{g_d}{s + g_d} (K_{tn} I_a - J_n \ddot{\theta}) \quad (20)$$

Disturbances can be calculated from  $I_a$  and  $\ddot{\theta}$ . However, measuring  $\dot{\theta}$  is much easier than measuring  $\ddot{\theta}$ . Hence, the optimized DC motor-based disturbance observer model in the S domain is depicted in fig. 5 and (21) represents the optimized disturbance torque estimation for practical use.

$$\hat{\tau}_d = \frac{g_d}{s + g_d} (K_{tn} I_a + g_d J_n \dot{\theta}) - g_d J_n \dot{\theta} \quad (21)$$

This estimated disturbance can be fed back into the system in order to achieve a robust control system.

##### B. Reaction Torque Observer

For a single degree of freedom system, interactive torque ( $\tau_{int}$ ) is zero. Hence, it is obvious that external torque ( $\tau_{ext}$ ) can be estimated from (22) if frictional components ( $B\dot{\theta}$  &  $\tau_{fric}$ ) and system parameters ( $K_t$  &  $J$ ) are known.

$$\tau_{ext} = \tau_d - (\tau_{int} + \tau_{fric} + B\dot{\theta} - \Delta K_t I_a + \Delta J \ddot{\theta}) \quad (22)$$

Researchers have introduced methods to estimate the above parameters using the disturbance observer [11].

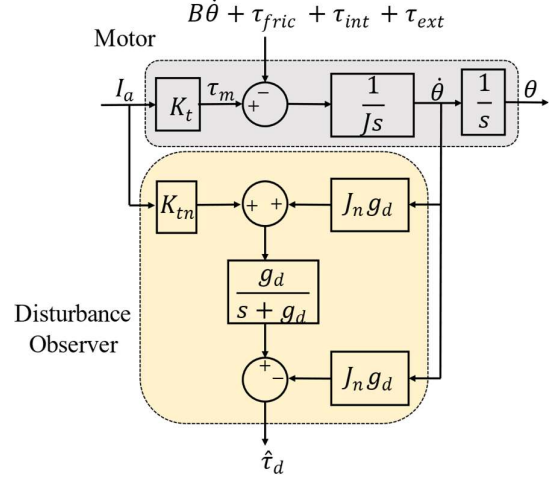


Fig 5. DC motor-based disturbance observer

Hence, external torque ( $\tau_{ext}$ ) can be estimated practically as in (23), where  $g_{rt}$  is the cutoff frequency of reaction torque observer LPF and that model is depicted in fig. 6.

External torque is the reaction torque that acts on the system. Hence, reaction torque can be accurately estimated from the above reaction torque observer without using a torque sensor.

For practical use, a single value is taken for both cutoff frequencies.

$$\hat{\tau}_{ext} = \frac{g_{rt}}{s + g_{rt}} [K_{tn} I_a + g_{rt} J_n \dot{\theta} - (\tau_{int} + \tau_{fric} + B\dot{\theta} - \Delta K_t I_a + \Delta J \ddot{\theta})] - g_{rt} J_n \dot{\theta} \quad (23)$$

## V. SIMULATIONS

The control system is constructed as shown in fig. 7.

The steering wheel position ( $\theta_s$ ) and rack position ( $\theta_r$ ) are exchanged as inputs to the rack and steering wheel respectively without scaling.

Steering wheel motor current, torque, velocity, and disturbance torque respectively  $I_{as}$ ,  $\tau_m$ ,  $\dot{\theta}_s$ , and  $\hat{\tau}_{ds}$ . Steering rack motor current, torque, velocity, and disturbance torque respectively  $I_{ar}$ ,  $\tau_{mr}$ ,  $\dot{\theta}_r$ , and  $\hat{\tau}_{dr}$ .

Robust motion control is attained by canceling out disturbances using the disturbance observer. Torques are estimated by a reaction torque observer. Hence, no torque sensors are used in this model.

The steering wheel and rack torque are exchanged as inputs to the rack and the steering wheel respectively. However, torque scaling ( $K_{scale}$ ) is used in this model in order to bring down the driver's steering effort to a comfortable level. The bilateral controller and motor parameters are listed in table 1.

Furthermore, driver dynamics, which were mentioned earlier in (10), are modeled on the steering wheel side.

Centering torque ( $\tau_{sa}$ ) is realized by modeling the front wheel and vehicle dynamics according to (7), (8) and, (9) by considering the vehicle dynamic data of the Volkswagen Golf V listed in table 2 for a constant vehicle speed [8].

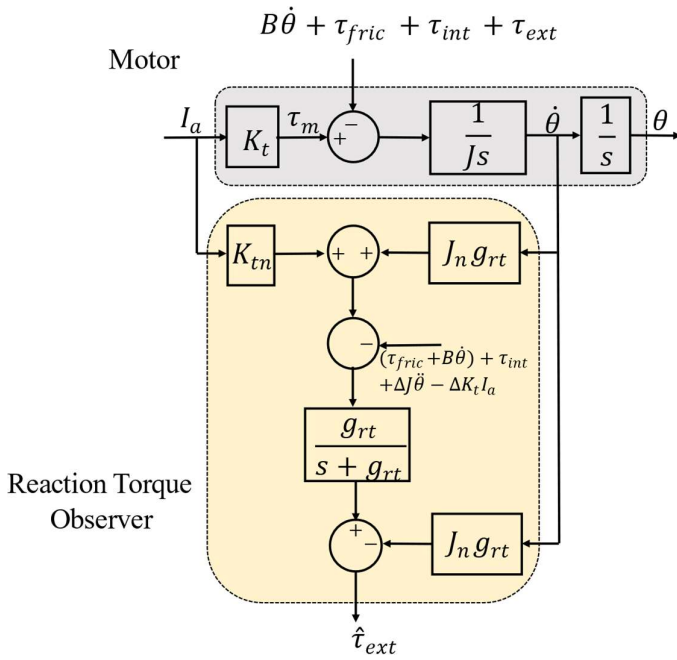


Fig 6. Reaction Torque Observer

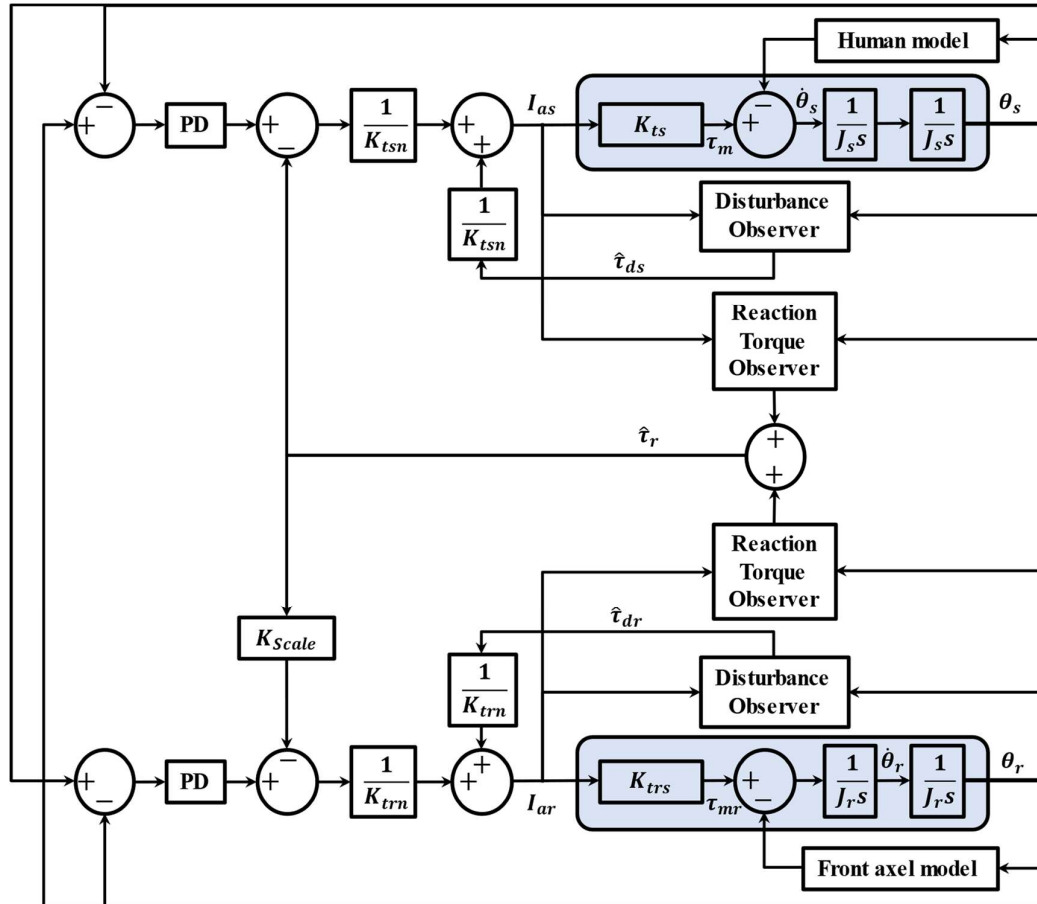


Fig 7. Simulated Steer by Wire Topology

A simulation was carried out by giving an input torque into the system via the steering wheel side and then position and reaction torque response of the steering wheel motor and rack motor were observed. Figure 8 shows the torque response of the steering wheel and rack motors to a step input. It is visible that torque at the steering wheel motor is scaled by the scale factor at the rack motor.

This system is applicable for all sorts of inputs as step input response correctly tracks the motion and forces.

Table 1. Bilateral controller and motor parameters

Parameter	Value	
$K_{ts}$	S.W.M torque coefficient	0.135 Nm/A
$K_{tsn}$	S.W.M nominal torque coefficient	0.135 N/A
$J_s$	S.W.M inertia	0.0000077kgm <sup>2</sup>
$J_{sn}$	S.W.M nominal inertia	0.000007 kgm <sup>2</sup>
$K_{tr}$	R.M torque coefficient	0.135 Nm/A
$K_{trn}$	R.M nominal torque coefficient	0.135 Nm/A
$J_r$	R.M inertia	0.00005 kgm <sup>2</sup>
$J_{rn}$	R.M nominal inertia	0.00001 kgm <sup>2</sup>
$K_{Ps}$	S.W.M controller proportional gain	100
$K_{Ds}$	S.W.M controller derivative gain	25
$K_{Pr}$	R.M controller proportional gain	750
$K_{Dr}$	R.M controller derivative gain	100
$g_{rt}$	Reaction torque observer LPF gain	100
$g_d$	Disturbance observer LPF gain	100
$k_{scale}$	Torque Scaling	20

Table 2. Vehicle parameters

Parameter	Value	
$c_{rw}$	Rear wheel cornering stiffness	118600 N/rad
$c_{fw}$	Front wheel cornering stiffness	118600 N/rad
$t_p$	Pneumatic tire trail	0.07 m
$t_m$	Mechanical tire trail	0.04 m
$l_{fw}$	Distance from COG to front	1.03 m
$l_{rw}$	Distance from COG to rear	1.55 m
$I_v$	Vehicle yaw moment inertia	2500 kgm <sup>2</sup>
$m_v$	Vehicle mass	1425 kg
$v$	Vehicle speed	90 km/h (25 m/s)
$\mu$	Dry road condition	0.85
$K_{ratio}$	Steering ratio	20:1

Figure 9 shows the position response to a step disturbance torque input. It shows a perfect match between the rack motor and the steering wheel motor positions.

Another simulation was carried out by giving a ramp signal as a disturbance input to the steering wheel motor. Figure 10 and 11 show the torque and position response. There too, the position is perfectly matched and torque scaling is successfully achieved.

Another simulation was carried out by making the vehicle speed 36 km/h and step input was given as earlier. According to fig. 12 and 13. There too, the position is perfectly matched and torque scaling is successfully achieved.

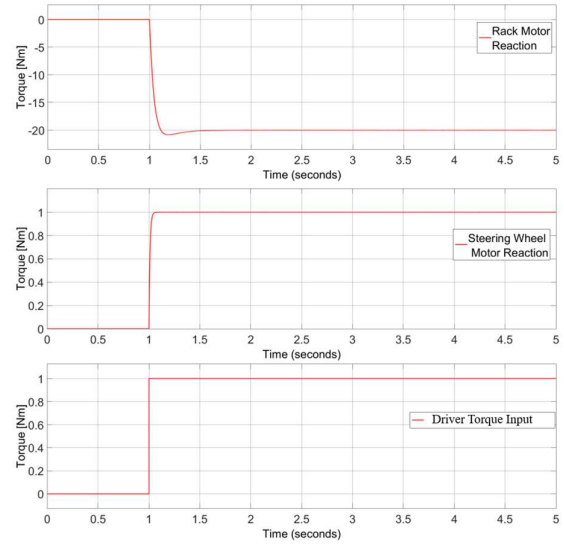


Fig 8. Torque response for step input at steering wheel

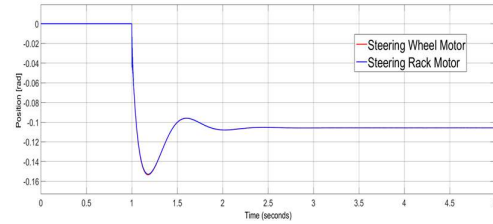


Fig 9. Position response for step input at steering wheel

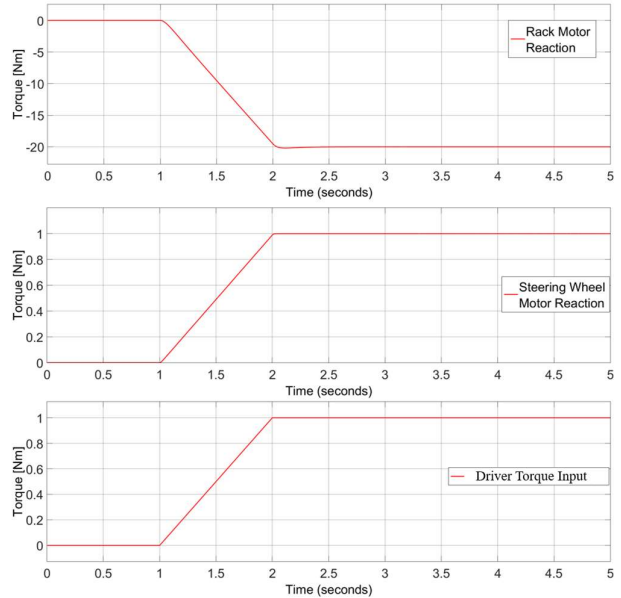


Fig 10. Torque response for ramp input at steering wheel

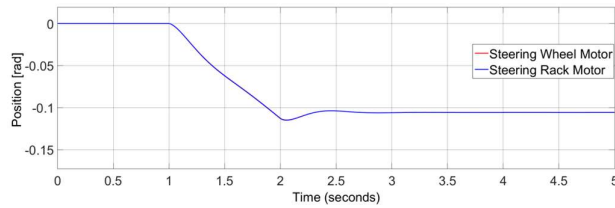


Fig 11. Position response for ramp input at steering wheel

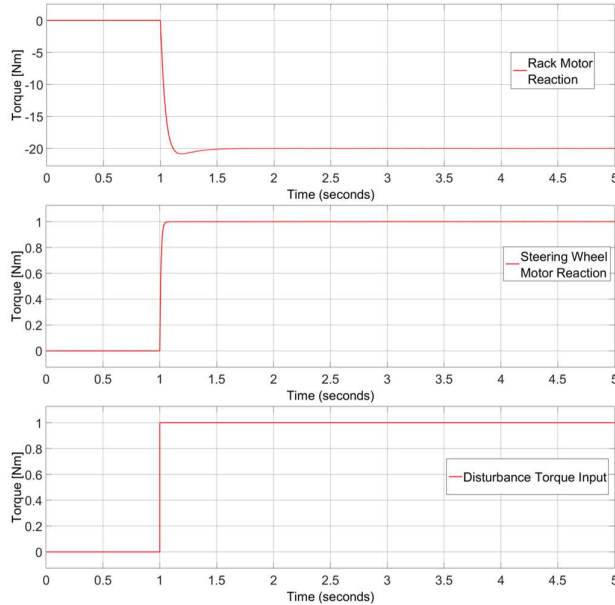


Fig 12. Torque response for step input at steering wheel at 36 km/h

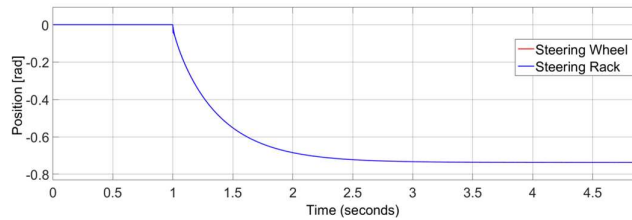


Fig 13. Position response for step input at steering wheel at 36 km/h

## VI. CONCLUSION

Using the analogy between the steering wheel column's dynamics and bilateral control criteria, a novel topology of the Sbw system, which is capable of surpassing the demerits of torque sensors as well as the demerits of other existing Sbw systems, has been proposed in this paper. The proposed system has been simulated using Volkswagen Golf V vehicle parameters on a fairly dry road. Obtained simulation results for various types of torque inputs as well as various vehicle speeds showed a satisfactory tracking performance.

Hence, it demonstrated the applicability of the proposed method.

## IV. ACKNOWLEDGMENT

The authors gratefully acknowledge the support provided by the Senate Research Committee, University of Moratuwa (SRC/LT/2020/21).

## REFERENCES

- [1] H. Zheng, J. Zhou, and B. Li, "Design of Adjustable Road Feeling Performance for Steering-by-Wire System," *SAE International Journal of Vehicle Dynamics, Stability, and NVH*, vol. 2, no. 2, pp. 121–134, Jun. 2018, doi: 10.4271/10-02-02-0008.
- [2] S. Asai, H. Kuroyanagi, S. Takeuchi, T. Takahashi, and S. Ogawa, "Development of a Steer-by-Wire System with Force Feedback Using a Disturbance Observer," SAE Technical Paper Series, Mar. 2004, doi: 10.4271/2004-01-1100.
- [3] C-J. Kim, J-H. Jang, S-K. Oh, J-Y. Lee, C-S. Han, and J. K. Hedrick, "Development of a control algorithm for a rack-actuating steer-by-wire system using road information feedback," Proceedings of the Institution of Mechanical Engineers, Part D: Journal of Automobile Engineering, vol. 222, no. 9, pp. 1559–1571, Sep. 2008, doi: 10.1243/09544070jauto825.
- [4] S. M. H. Fahami, H. Zamzuri, and S. A. Mazlan, "Development of Estimation Force Feedback Torque Control Algorithm for Driver Steering Feel in Vehicle Steer by Wire System: Hardware in the Loop," *International Journal of Vehicular Technology*, vol. 2015, pp. 1–17, 2015, doi: 10.1155/2015/314597.
- [5] A. M. H. S. Abeykoon, W. M. T. G. Wijewardhana, E. H. Senevirathne, and K. D. M. Jayawardhana, "Vibration suppression of force controllers using disturbance observers," *Vibration Control and Actuation of Large-Scale Systems*, pp. 57–89, 2020, doi: 10.1016/b978-0-12-821194-6.00003-2.
- [6] A. M. H. S. Abeykoon and K. Ohnishi, "Realization of Virtual Master Manipulator Using Bilateral Control," 2006 4th IEEE International Conference on Industrial Informatics, 2006, pp. 833–838, doi: 10.1109/INDIN.2006.275670.
- [7] A. M. H. S. Abeykoon and K. Ohnishi, "Implementation of pedal feeling for Brake By Wire system using bilateral control," 2008 IEEE International Symposium on Industrial Electronics, 2008, pp. 1347–1352, doi: 10.1109/ISIE.2008.4677132.
- [8] Dieter Schramm, Manfred Hiller, and R. Bardini, *Vehicle Dynamics : Modeling and Simulation*. Berlin, Heidelberg: Springer Berlin Heidelberg, 2018.
- [9] K. Ohnishi, M. Shibata and T. Murakami, "Motion control for advanced mechatronics," in *IEEE/ASME Transactions on Mechatronics*, vol. 1, no. 1, pp. 56–67, March 1996, doi: 10.1109/3516.491410.
- [10] H. R. Senevirathne, A. M. H. S. Abeykoon and M. B. Pillai, "Disturbance rejection analysis of a disturbance observer based velocity controller," 2012 IEEE 6th International Conference on Information and Automation for Sustainability, 2012, pp. 59–64, doi: 10.1109/ICIAFS.2012.6419882.
- [11] W. M. T. G. Wijewardhana, E. H. Senevirathne and A. M. H. S. Abeykoon, "Iterative Approach for Parameter Estimation in DC Motor Based Motion Systems," 2020 IEEE 29th International Symposium on Industrial Electronics (ISIE), 2020, pp. 134–141, doi: 10.1109/ISIE45063.2020.9152500.